symmetry

MDPI

Article

Unified Inflation and Late-Time Accelerated Expansion with Exponential and R^2 Corrections in Modified Gravity

Luis Granda

Departamento de Fisica, Universidad del Valle, Cali 25360, Colombia; luis.granda@correounivalle.edu.co

Received: 9 April 2020; Accepted: 6 May 2020; Published: 9 May 2020

check for updates

Abstract: Modified gravity models with and exponential function of curvature and R^2 corrections are proposed. At low curvature, the model explains the matter epoch and the late time accelerated expansion while at the inflation epoch the leading term is R^2. At $R \to 0$ the cosmological constant disappears, giving unified description of inflation and dark energy in pure geometrical context. The models satisfy the stability conditions, pass local tests and are viable in the (r, m)-plane, where the trajectories connect the saddle matter dominated critical point ($r = -1$, $m = 0$) with the late time de Sitter attractor at $r = -2$ and $0 < m \leq 1$. Initial conditions were found, showing that the density parameters evolve in a way consistent with current cosmological observations, predicting late time behavior very close to the ΛCDM with future universe evolving towards the de Sitter attractor.

Keywords: modified gravity; inflation; dark energy

1. Introduction

The possibilities of unification of the early time inflationary era with late time accelerated expansion of the universe is one of the attractive facts of modified gravity theories; this captured the attention of the researchers in this field. This approach, based on geometrical grounds, avoids the introduction of additional degrees of freedom for the inflation or dark energy.

The modified gravity models represent an appealing alternative to a dynamical explanation of dark energy (for review see [1–4]), despite the success of the cosmological constant as the source of dark energy, but which is clouded by the known fine tuning problem. These theories introduce additional non-linear corrections to the Einstein model, which are subject to local systems tests and cosmological observational constraints that determine the viability of the model (see [5–11] for reviews). A variety of models for modified gravity were proposed and some of them are [6,12–32]. Models that can satisfy both cosmological and local gravity constraints were proposed in [31,33–37], and exact cosmological solutions were studied in [38–44]. Modified gravity with arbitrary function of the 4-dimensional Gauss-Bonnet invariant was introduced in [45–47]. There are also models that attempt to unify early time inflation with late time acceleration, among which we can highlight: [15] in which negative and positive powers of curvature were introduced in order to unify inflation and cosmic acceleration, in [48] an extension of the Hu-Sawyki model [31] was proposed that includes inflation and late-time accelerated expansion, in [49] a modified gravity that unifies power-law curvature inflation with late-time ΛCDM epoch was considered, in [36] a class of exponential modified gravity models was introduced, in which the inflation and accelerated expansion are present, a simple modified model with exponential gravity was considered in [37,50], a model with exponential and logarithmic corrections was considered in [51] and constant roll inflation with exponential modified gravity was studied in [52]. Unified models of inflation and dark energy with modified Gauss-Bonnet contribution were studied in [45–47,53,54]. In [55] a comprehensive study of the cosmological constraints for general $f(R)$ theory was performed, where a classification of $f(R)$ models was proposed, depending on the existence of the standard matter era and on the final accelerated state. The viability of several models was also analyzed by using the autonomous system approach. In [56], local and cosmological constraints are discussed and the evolution of matter density perturbations was studied. A dynamical analysis and study of critical points for locally anisotropic cosmological models of modified gravity were carried out in [57,58].

The aim of this paper is to propose a simple viable model of $f(R)$ gravity that consistently describes both the inflationary epoch and the late time accelerated expansion of the universe, while satisfies the stringent local gravity constraints. This model contains a new exponential gravity correction that gives compatible with observations description of the cosmic evolution, mimicking the ΛCDM model, and R^2 term [32] that becomes relevant at high curvature and gives successful explanation of the early-time inflation. The viability of the model is shown in the (m, r) diagram which describes trajectories connecting the matter dominated saddle point at $r = -1$, $m = 0$ with late-time de Sitter attractor at $r = -1$ and $0 < m \leq 1$. The model also satisfies the more stringent local gravity constraints.

This paper is organized as follows. In Section 2 we present the general features of the $f(R)$ models, including the autonomous system and the relevant critical points for our study in terms of the (r, m) parameters. In Section 3 we present the model, showing the conditions for viability and its trajectories in the (r, m)-plane, including some numerical cases of cosmic evolution. In Section 4 we present some discussion.

2. Field Equations

The modified gravity can be the described by the following action

$$S = \int d^4x\sqrt{-g}\left[\frac{1}{2\kappa^2}f(R) + \mathcal{L}_m\right] \tag{1}$$

where $\kappa^2 = 8\pi G$ and $\mathcal{L}_m$ is the Lagrangian density for the matter component which satisfies the usual continuity equation. The equation of motion is given by

$$f_{,R}(R)R_{\mu\nu} - \frac{1}{2}g_{\mu\nu}f(R) + \left(g_{\mu\nu}\Box - \nabla_\mu\nabla_\nu\right)f_{,R}(R) = \kappa^2 T^{(m)}_{\mu\nu} \tag{2}$$

where $T^{(m)}_{\mu\nu}$ is the matter energy-momentum tensor assumed as

$$T^{m}_{\mu\nu} = (\rho + p)\, u^\mu u^\nu + p g_{\mu\nu}$$

and $f_{,R} \equiv \frac{df}{dR}$. The trace of Equation (2) gives

$$Rf_{,R}(R) - 2f(R) + 3\Box f_{,R}(R) = \kappa^2 T^{(m)} = \kappa^2\left(3p - \rho\right) \tag{3}$$

Extracting the time and spatial components of Equation (2) gives by the expressions

$$3H^2 f_{,R} = \frac{1}{2}\left(Rf_{,R} - f\right) - 3H\dot{f}_{,R} + \kappa^2\rho \tag{4}$$

and

$$-2\dot{H}f_{,R} = \ddot{f}_{,R} - H\dot{f}_{,R} + \kappa^2\left(\rho + p\right) \tag{5}$$

where dot represents derivative with respect to cosmic time. The effective equation of state (EoS) from these expressions is

$$w_{eff} = -1 - \frac{2\dot{H}}{3H^2} = -1 + \frac{\ddot{f}_{,R} - H\dot{f}_{,R} + \kappa^2(\rho + p)}{\frac{1}{2}(Rf_{,R} - f) - 3H\dot{f}_{,R} + \kappa^2\rho}, \tag{6}$$

where ρ and p include both matter and radiation components, i.e., $\rho = \rho_m + \rho_r$ and $p = p_m + p_r$. The viability conditions begin with the stability which demands that

$$f_{,R} > 0, \quad f_{,RR} > 0 \tag{7}$$

where the first condition is necessary to avoid change of sign in the effective Newtonian coupling, and the second is necessary in order to avoid tachyonic behavior of the scalaron and is also a condition of stability under perturbations, especially at the matter dominated epoch. In fact, the scalar particle associated with $f(R)$, dubbed scalaron with mass

$$M^2 = \frac{1}{3}\left(\frac{f_{,R}}{f_{,RR}} - R\right) \tag{8}$$

which in matter epoch or in the regime $M^2 >> R$, when $Rf_{,RR} << 1$ and $f_{,R} \simeq 1$ can be reduced to

$$M^2 \simeq \frac{1}{3f_{,RR}}, \tag{9}$$

which requires $f_{,RR} > 0$. Apart from that, the model must be compatible with the observational evidence at both local and cosmological scales. The mass M plays an important role in local gravity constraints since it defines the range of the force mediated by the scalaron which determines the Compton wavelength $\lambda_C = 2\pi M^{-1}$. If ℓ is the typical size of a local gravitational system, then the local gravity constraints on $f(R)$ are satisfied whenever $\ell >> \lambda_C$ or $M\ell >> 1$ [55,56]. On the other hand, to demonstrate the viability of modified gravity as cosmological model it is useful to consider the autonomous system with the following dimensionless variables that can be obtained from Equation (4) [55] (we will use indistinctly $f_{,R}$ or $F = f_{,R}$)

$$x = -\frac{\dot{F}}{HF}, \quad y = -\frac{f}{6H^2F}, \quad z = \frac{R}{6H^2} = \frac{\dot{H}}{H^2} + 2, \quad w = \frac{\kappa^2\rho_r}{3H^2F}, \quad \Omega_m = \frac{\kappa^2\rho_m}{3H^2F} \tag{10}$$

which lead to the following dynamical system

$$x + y + z + w + \Omega_m = 1 \tag{11}$$

$$\frac{dx}{dN} = x^2 - xz - 3y - z + w - 1 \tag{12}$$

$$\frac{dy}{dN} = xy + \frac{xz}{m} - 2y(z-2) \tag{13}$$

$$\frac{dz}{dN} = -\frac{xz}{m} - 2z(z-2) \tag{14}$$

$$\frac{dw}{dN} = xw - 2zw \tag{15}$$

where $N = \ln a$, $w = \Omega_r$ is the density parameter of the radiation component, and m is given by

$$m = \frac{Rf_{,RR}}{f_{,R}}. \tag{16}$$

Along with the parameter m there is another useful parameter r defined as

$$r = -\frac{Rf_{,R}}{f}. \tag{17}$$

These parameters are useful to analyze the cosmological viability of $f(R)$ models and characterize the deviation of a given $f(R)$ model from the standard ΛCDM model, which corresponds to the line $m = 0$. In terms of the dynamical variables the effective EoS (6) is written as

$$w_{eff} = -\frac{1}{3}\left(2z - 1\right), \tag{18}$$

while the dark energy equation of state from (4) and (5) can be written as [55,56]

$$w_{DE} = -\frac{1}{3}\frac{2z - 1 + (F/F_0)w}{1 - (F/F_0)(1 - x - y - z)}, \tag{19}$$

where F_0 is the current value of $f_{,R}$.

The critical points of the dynamical system (11)–(15), that are the solutions of the equations ([55,56])

$$\frac{dx}{dN} = 0, \; ... \; \frac{dw}{dN} = 0, \tag{20}$$

allow analyzing asymptotic cosmological solutions of the model (1) and their stability properties. Among the solutions of the system (20) there are three important critical points that we will consider to analyze the viability of our models (in this analysis we do not consider the contribution of radiation, which does not change the stability properties of the critical points).

The first critical point corresponds to scaling solutions which include the matter dominated era, has the following coordinates in terms of the parameter m

$$P_S = (x_c, y_c, z_c) = \left(\frac{3m}{1+m}, -\frac{1+4m}{2(1+m)^2}, \frac{1+4m}{2(1+m)}\right), \tag{21}$$

with eigenvalues

$$EV(P_S) : \left(3(1+m'), \frac{-3m \pm \sqrt{m(256m^3 + 160m^2 - 31m - 16)}}{4m(m+1)}\right), \tag{22}$$

where m is given by (16) and prime represents derivative with respect to r. At this point the matter density parameter and the effective EoS take the form

$$\Omega_m = 1 - \frac{m(7+10m)}{2(1+m)^2}, \;\; w_{eff} = -\frac{m}{1+m}, \tag{23}$$

The second point has the coordinates

$$P_{deS} = (x_c, y_c, z_c) = (0, -1, 2), \tag{24}$$

with eigenvalues

$$EV(P_{deS}) : \left(-3, -\frac{3}{2} \pm \frac{\sqrt{25 - 16/m(r=-2)}}{2}\right), \tag{25}$$

and lead to the de Sitter solution with

$$\Omega_m = 0, \quad w_{eff} = -1 \tag{26}$$

The third critical point, that leads to accelerated expansion scenarios, has the coordinates

$$P_C = (x_c, y_c, z_c) = \left(\frac{2(1-m)}{1+2m}, \frac{1-4m}{m(1+2m)}, -\frac{(1-4m)(1+m)}{m(1+2m)} \right), \tag{27}$$

with the eigenvalues

$$EV(P_C) : \left(-4 + \frac{1}{m}, \frac{2-3m-8m^2}{m(1+2m)}, -\frac{2(m^2-1)(1+m')}{m(1+2m)} \right). \tag{28}$$

The matter density parameter and effective EoS corresponding to this point are

$$\Omega_m = 0, \;\; w_{eff} = \frac{2-5m-6m^2}{3m(1+2m)}, \tag{29}$$

From the coordinates y and z for the points P_S and P_C it can be seen that they are connected by the line $m(r) = -1 - r$, where the relation

$$r(N) = \frac{z(N)}{y(N)} \tag{30}$$

is used.

From (21) follows that the matter dominated point corresponds to (r, m)=$(-1, 0)$. The existence of a viable saddle matter era requires $m(r \to -1) > 0$ and $-1 < dm/dr(r \to -1) \leq 0$. This last condition implies that all the $m(r)$ trajectories must be between the lines $m = 0$ and $m = -r - 1$. In order to be viable, the trajectory of a given $f(R)$ model in the (r, m) plane should be such that it contains the matter dominated point $P_M = (-1, 0)$ and starting from P_M intersects the line $r = -2$ in the region $0 < m \leq 1$ [55]. The ΛCDM model, for instance, connect the points $P_M = (-1, 0)$ and $P_{dS} = (-2, 0)$. There are also viable trajectories connecting the saddle matter point $P_M = P_S(m \to 0)$ with the curvature dominated point that leads to stable accelerated expansion P_C, whenever $m' > -1$.

3. The Models

The following model, as will be shown satisfies all above discussed conditions of stability and viability

$$f(R) = R - 2\lambda_1 \mu^2 e^{-\left(\frac{\mu^2}{R}\right)^{\eta}} + \frac{\lambda_2}{\mu^2} R^2 \tag{31}$$

where the dimensionless constants η, λ_1 and λ_2 are positive, and $0 < \eta \leq 1$. This function is well defined for any R and describes the physical regimes related to the crucial cosmological epochs epochs of the universe: the inflationary regime where the relevant contribution comes from the R^2 Starobinsky term and the small curvature regime covering from the matter era to the current stage of accelerated expansion, where gravity is described mainly by the first two terms in (31). The Lagrangian composed of

$$R + \frac{\lambda_2}{\mu^2} R^2, \tag{32}$$

which is the dominant sector of the model (31) for large curvature, typical of the inflationary epoch, gives the well known and still consistent with observational data Starobinsky inflation. Hence, these two corrections are of different nature and are introduced for different purposes. Then to analyze the viability of the model to explain the late time accelerated expansion, the R^2 term should be irrelevant, which imposes restrictions on the parameter λ_2. In fact the scale μ^2 was introduced in the last term with the sole objective to make λ_2 dimensionless, since at the end λ_2 must satisfy the restrictions imposed by the curvature at the inflationary period. The properties of the model (31) must be reflected in the behavior of the autonomous system, as we show below. First we note that the exponential function satisfies the limits

$$\lim_{R\to 0} e^{-\left(\frac{\mu^2}{R}\right)^\eta} = 0, \quad \lim_{R\to \infty} e^{-\left(\frac{\mu^2}{R}\right)^\eta} = 1. \tag{33}$$

The first limit allows the existence of flat spacetime solutions and the second is necessary for consistency with high redshift CMB observations.

To check the stability conditions (7) we analyze the corresponding expressions for $f_{,R}$ and $f_{,RR}$

$$f_{,R} = 1 - 2\lambda_1\eta\left(\frac{\mu^2}{R}\right)^{1+\eta} e^{-\left(\frac{\mu^2}{R}\right)^\eta} + \frac{2\lambda_2 R}{\mu^2}, \tag{34}$$

$$f_{,RR} = \frac{2\eta\lambda_1}{\mu^2}\left(\frac{\mu^2}{R}\right)^{2+\eta}\left[1+\eta-\eta\left(\frac{\mu^2}{R}\right)^\eta\right] e^{-\left(\frac{\mu^2}{R}\right)^\eta} + \frac{2\lambda_2}{\mu^2}. \tag{35}$$

The condition $f_{,R} > 0$ can be easily meet under the assumption $\mu^2 < R$ and taking into account that $0 < \eta \leq 1$. Since the last term in (34) is positive and the R-dependent terms are always less than 1, it can be satisfied under the following restriction on λ_1

$$\lambda_1 < \frac{1}{2\eta}. \tag{36}$$

From (35) follows that $f_{,RR} > 0$ is always true for $\mu^2 < R$ and $0 < \eta \leq 1$. This is compatible with the criteria we will use below to redefine the stability conditions, by setting λ_1 such that the de Sitter critical point takes place at $R = R_1$.

The r and m parameters for the model (31), that determine its cosmological viability, are obtained from (17) and (16) respectively and are given by

$$r = -\frac{\frac{R}{\mu^2}\left(2\lambda_1\frac{R}{\mu^2} - 2\eta\lambda_2 e^{-\left(\frac{\mu^2}{R}\right)^\eta}\left(\frac{\mu^2}{R}\right)^{\eta+1} + 1\right)}{\frac{R}{\mu^2} + \lambda_1\left(\frac{R}{\mu^2}\right)^2 - 2\lambda_2 e^{-\left(\frac{\mu^2}{R}\right)^\eta}} \tag{37}$$

and

$$m = \frac{2\lambda_1 e^{\left(\frac{\mu^2}{R}\right)^\eta}\left(\frac{R}{\mu^2}\right)^2 + 2\eta\lambda_2\left(\frac{\mu^2}{R}\right)^\eta\left(1+\eta\left(1-\left(\frac{\mu^2}{R}\right)^\eta\right)\right)}{\frac{R}{\mu^2}e^{\left(\frac{\mu^2}{R}\right)^\eta} + 2\lambda_1\left(\frac{R}{\mu^2}\right)^2 e^{\left(\frac{\mu^2}{R}\right)^\eta} - 2\eta\lambda_2\left(\frac{\mu^2}{R}\right)^\eta}. \tag{38}$$

where the expressions for $f_{,R}$ and $f_{,RR}$ from (34) and (35) were used.

To analyze the stability at the de Sitter point $0 < m(r=-2) \leq 1$, we fix λ_1 in such a way that the de Sitter point $r = -2$ takes place at $R = R_1$. From (37) it is found

$$\lambda_1 = \frac{\frac{R_1}{\mu^2}e^{\left(\frac{\mu^2}{R_1}\right)^\eta}}{2\left[2-\eta\left(\frac{\mu^2}{R_1}\right)^\eta\right]}. \tag{39}$$

Please note that this value does not depend on λ_2 because de de Sitter solution is automatically satisfied by the R^2-model. The restriction $\lambda_1 > 0$ can be solved by imposing

$$\left(\frac{\mu^2}{R_1}\right)^\eta < \frac{2}{\eta} \tag{40}$$

And for the stability condition at the de sitter point $0 < m(r = -2) \leq 1$, using the above value for $\lambda - 1$, leads to

$$0 < \frac{\eta\left(\frac{\mu^2}{R_1}\right)^\eta\left(1+\eta\left(1-\left(\frac{\mu^2}{R_1}\right)^\eta\right)\right)+2\lambda_2\frac{R_1}{\mu^2}\left(2-\eta\left(\frac{\mu^2}{R_1}\right)^\eta\right)}{2\left(1-\eta\left(\frac{\mu^2}{R_1}\right)^\eta\right)+2\lambda_2\frac{R_1}{\mu^2}\left(2-\left(\frac{\mu^2}{R_1}\right)^\eta\right)} \leq 1 \tag{41}$$

This inequality cannot be solved explicitly in terms of R_1, but it we choose the parametrization

$$\frac{\mu^2}{R_1} = \left(\frac{1}{p\eta}\right)^{1/\eta}, \quad p > 1 \tag{42}$$

which satisfies (40), then the inequality (41) becomes

$$0 < \frac{\eta\left(\frac{1}{p\eta}\right)^{1+1/\eta}(1+\eta-1/p)+2\lambda_2(2-1/p)}{2\left(\frac{1}{p\eta}\right)^{1/\eta}(1-1/p)+2\lambda_2(2-1/p)} \leq 1 \tag{43}$$

that is satisfied by

$$p \geq \frac{\eta+3}{4} + \frac{1}{4}\sqrt{\eta^2+6\eta+1}, \quad 0 < \eta \leq 1. \tag{44}$$

In fact, given that $0 < \eta \leq 1$, this inequality is always satisfied by any $p \geq 1 + 1/\sqrt{2}$ which is consistent with (42).

Turning to the stability conditions and taking into account λ_1 from (39) and R_1 from (42), we find after replacing in (34)

$$f_{,R} = 1 - \frac{e^{\frac{1}{p\eta}-\left(\frac{\mu^2}{R}\right)^\eta}}{(2p-1)(p\eta)^{1/\eta-1}}\left(\frac{\mu^2}{R}\right)^{1+\eta} + 2\lambda_2\frac{R}{\mu^2} \tag{45}$$

as $\lambda_2 > 0$, then a sufficient condition to satisfy the inequality $f_{,R} > 0$ is

$$\frac{e^{\frac{1}{p\eta}-\left(\frac{\mu^2}{R}\right)^\eta}}{(2p-1)(p\eta)^{1/\eta-1}}\left(\frac{\mu^2}{R}\right)^{1+\eta} < 1. \tag{46}$$

From the fact that $R > R_1$ follows that $\mu^2/R < \mu^2/R_1$ or

$$\frac{\mu^2}{R} < \left(\frac{1}{p\eta}\right)^{1/\eta},$$

then the inequality (46) also takes place if we assume the maximum value for μ^2/R, which reduces to

$$(2p-1)(p\eta)^{2/\eta} > 1 \tag{47}$$

which takes place if additionally to $p > 1$, we impose the restriction $p\eta \geq 1$. For the second derivative $f_{,RR}$ we obtain

$$f_{,RR} = \frac{1}{(2p-1)\mu^2} (p\eta)^{1+1/\eta} e^{\frac{1}{p\eta} - \left(\frac{\mu^2}{R}\right)^\eta} \left(\frac{\mu^2}{R}\right)^{2+\eta} \left(1 + \eta - \eta \left(\frac{\mu^2}{R}\right)^\eta\right) + \frac{2\lambda_2}{\mu^2} \tag{48}$$

And the stability condition $f_{,RR}$ is automatically satisfied since $p > 1$ and $R > \mu^2$ (we can also use the maximum value of μ^2/R coming from the inequality $R > R_1$ to find that $1 + \eta - 1/p > 0$, which leads to $f_{,RR} > 0$). Thus, we found the conditions for stability without compromising the constant λ_2 which will be useful in adjusting the Starobinsky R^2 term with the scale of inflation. It is worth noticing that the stability condition $f_{,RR} > 0$ holds for any $R > R_1$, and there are not any instability problems related to the matter epoch and at local systems scales. Note also that the stability conditions derived after fixing λ_1 maintain the consistency with the general stability conditions derived for $f_{,R}$ and $f_{,RR}$ given by the expressions (34) and (35) respectively. The restriction (36) on λ_1 can be satisfied assuming, for instance, $p\eta = 1$ (i.e., $\mu^2/R_1 = 1$) one finds

$$\eta < \frac{2}{e+1}. \tag{49}$$

To analyze the viability of the model in the (r, m)-plane we resort to the parametric plot of some trajectories, since m cannot be expressed analytically in terms of r. Using (37) and (38) and defining the variable $y = R/\mu^2$ with de Sitter value $y_1 = R_1/\mu^2$ (see (42)) we can write the corresponding expressions for r and m as follows

$$r = -\frac{(2p-1)\,(1+2\lambda_2 y)\, y^{\eta+1} - (p\eta)^{1+1/\eta}\, e^{\frac{1}{p\eta} - \frac{1}{y^\eta}}}{(2p-1)\,(1+\lambda_2 y)\, y^{\eta+1} - p\,(p\eta)^{1/\eta}\, y^\eta e^{\frac{1}{p\eta} - \frac{1}{y^\eta}}} \tag{50}$$

$$m = \frac{2\lambda_2(2p-1)y^{2\eta+2} + (p\eta)^{1+1/\eta}\,((1+\eta)\, y^\eta - \eta)\, e^{\frac{1}{p\eta} - \frac{1}{y^\eta}}}{(2p-1)\,(1+2\lambda_2 y)\, y^{2\eta+1} - (p\eta)^{1+1/\eta}\, y^\eta e^{\frac{1}{p\eta} - \frac{1}{y^\eta}}} \tag{51}$$

where we used the expression for λ_1 from (39). It can be confirmed that at $y = (p\eta)^{1/\eta}$, r takes the value $r = -2$. To simplify the numerical analysis, in what follows we assume the restriction

$$p\eta = 1, \tag{52}$$

that satisfies all above restrictions and, according to (42), gives $R_1 = \mu^2$.

On the other hand, the value of λ_2 must be chosen in such a way that

$$\frac{\lambda_2}{\mu^2} \sim \frac{6}{M^2} \tag{53}$$

where $M \sim 10^{13} Gev$, which is the typical value required for inflation. If R_i is the typical curvature during inflation, then the coefficient λ_2/μ^2 should be of the order of

$$\lambda/\mu^2 \sim 1/R_i$$

to ensure that in the small curvature regime, when $R << R_i$, it is verified that

$$R >> \frac{R^2}{R_i}, \tag{54}$$

necessary to avoid the effect of the R^2-term in the small curvature regime. Thus, for the model (31) the physical criteria to establish the value of λ_2 involves the curvature (mass) scale μ. At the same time, this scale is set so that local gravity constraints are satisfied. In any case since, after the restriction (52), the de Sitter curvature satisfies $R_1 = \mu^2$, then this scale should be smaller than the current curvature $R_0 \sim H_0^2$, i.e., $\mu^2 < H_0^2$, which implies, according to (53), that

$$\lambda_2 < \frac{H_0^2}{6M^2} \sim 10^{-112} \tag{55}$$

In Figure 1 we present some trajectories in the (r, m)-plane. The model contains the matter dominated point $P_M = (-1, 0)$ and cosmologically viable trajectories that connect the matter era with the final de Sitter attractor at $r = -2$. As can be seen from Figure 1 the value of λ_2 is such that it avoids the effects of the R^2 term during the matter era. Nevertheless numerical calculations show that the curves in Figure 1 practically remain unchanged for any $\lambda_2 < 10^{-7}$, which reflects the fact that the scale μ is not relevant for the cosmological trajectories in the (r, m)-plane. The real stringent restrictions on μ, and therefore on λ_2 through (53), come from the local gravity tests.

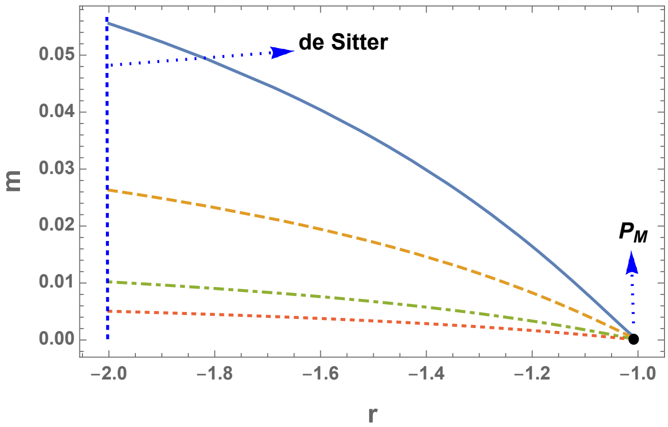

Figure 1. Trajectories in the (r, m)-plane for four different scenarios with $\lambda_2 = 10^{-7}$ and $(\eta, p) = (0.1, 10)$ (solid line), $(0.05, 20)$ (dashed), $(0.02, 50)$ (dotdashed), $(0.01, 100)$ (dotted). In all cases $p\eta = 1$, but for smaller η and larger p the trajectories become closer to ΛCDM. All trajectories connect the matter dominated saddle point P_M with the late time de Sitter attractor at $r = -2$ with $0 < m < 1$.

Local Gravity Constraints.

The effective mass corresponding to the modified gravity $f(R)$ model is given by

$$M^2 = \frac{R}{3}\left(\frac{f_{,R}}{Rf_{,RR}} - 1\right) = \frac{R}{3m}(1 - m)\,. \tag{56}$$

This mass characterizes the range of the force mediated by the scalaron and defines the Compton wavelength $\lambda_C = 2\pi/M$. To avoid the propagation of this scalar degree of freedom and satisfy the local gravity constraints, this Compton length must be negligible small compared to the typical size of the system ℓ, $\lambda_C << \ell$. Thus, to satisfy the local gravity constraints it is necessary that

$$M\ell >> 1. \tag{57}$$

If we use the approximation for the local curvature $R_s \sim \ell^{-2}$, then using this in (56) we can write

$$M^2 \sim \frac{\ell^{-2}}{3m}(1 - m) \tag{58}$$

then from (57) it follows that

$$\frac{\sqrt{1-m}}{\sqrt{3m}} >> 1 \quad \Rightarrow \quad m << 1, \tag{59}$$

which gives from (56)

$$M^2 \simeq \frac{R}{3m}. \tag{60}$$

This allows us to write the constraint (57) as

$$m(R_s) << \ell^2 R_s. \tag{61}$$

Making use of the relationship $R \sim H^2 \sim 8\pi G\rho$ applied to the current universe (R_0, ρ_0) and to the local structure (R_s, ρ_s), we can write $R_s \sim H_0^2 \rho_s/\rho_0$ and the above constraint becomes [56]

$$m(R_s) << \frac{\rho_s}{\rho_0}\left(\frac{\ell}{H_0^{-1}}\right)^2. \tag{62}$$

For the solar system with $\rho_s \sim 10^{-23}$ gr/cm^3 and $\ell \sim 10^{13}$ cm one finds that $m << 10^{-24}$, where we used $H_0^{-1} \sim 10^{28}$ cm.

Applied to the model (31) the local gravity constraints can be addressed using the representation for m given by (51). For the solar system one has $y_s = R_s/\mu^2$, where $R_s \simeq 10^6 H_0^2$. For the parameters η and p used in Figure 1, we will set $\mu^2 = 10^{-16} H_0^2$, which gives $y_s = 10^{22}$ and $\lambda_2 \sim 10^{-127}$ (assuming $m \sim 10^{13} Gev$ in (53))

$$\begin{aligned}
(\eta = 0.1,\ p = 10) \quad &\Rightarrow m = 9.8 \times 10^{-26} \\
(\eta = 0.05,\ p = 20) \quad &\Rightarrow m = 5.3 \times 10^{-25} \\
(\eta = 0.02,\ p = 50) \quad &\Rightarrow m = 7 \times 10^{-25} \\
(\eta = 0.01,\ p = 100) \quad &\Rightarrow m = 4.5 \times 10^{-25}
\end{aligned}$$

Hence, the model (31) can pass solar system tests, assuming $\mu \sim 10^{-8} H_0$ for the viable trajectories depicted in Figure 1. If we consider larger values of η then the results for local systems improve as shown bellow.

$$\begin{aligned}
(\eta = 1/5,\ p = 5) \quad &\Rightarrow m = 1.4 \times 10^{-27} \\
(\eta = 1/4,\ p = 4) \quad &\Rightarrow m = 1.5 \times 10^{-28} \\
(\eta = 1/3,\ p = 3) \quad &\Rightarrow m = 3.4 \times 10^{-30} \\
(\eta = 1/2,\ p = 2) \quad &\Rightarrow m = 1.4 \times 10^{-33}
\end{aligned} \tag{63}$$

It is worth noting that the above numerical values for local restrictions on m can be obtained for $\lambda_2 \lesssim 10^{-55}$, even though λ_2 is subject to the restriction (53) which results in much smaller values than this limit.

In Figure 2 we present the evolution of the density parameters for the radiation Ω_r, matter Ω_m and the geometrical dark energy Ω_{DE}, with parameters η and p that satisfy cosmological constraints. Since there is no explicit expression for $m(r)$, we used a polynomial fit to the paths depicted in Figure 1. Taking, for instance, the cosmological scenario with $\mu = 0.01$ and $p = 100$, the corresponding trajectory in Figure 1 can be approximated by the following function of the dynamical variables $y[t]$ and $z[t]$ ($t = -\ln(1+z)$)

$$m = c_0 + c_1\sqrt{-\frac{z[t]}{y[t]}} + c_2\frac{z[t]}{y[t]} \tag{64}$$

with

$$c_0 = -0.0339961',\ \ c_1 = 0.0495968',\ \ c_2 = 0.0155756'$$

where ($'$) represents more digits taken into account for the numerical calculations.

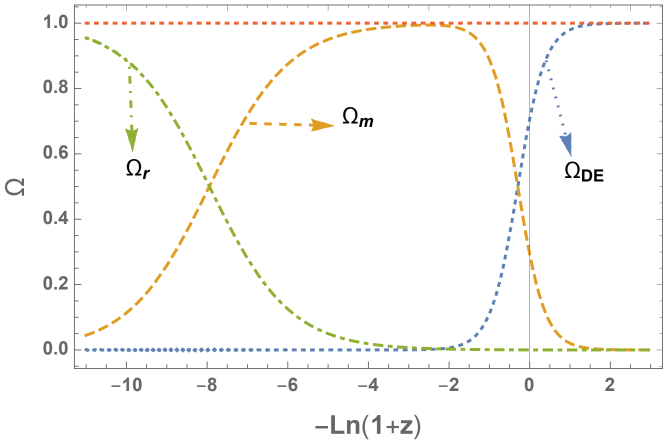

Figure 2. The cosmic evolution of the density parameters for matter, radiation and dark energy for the model (31). In this example we take the path of Figure 1 for the parameters $\eta = 0.01$, $p = 100$ and $\lambda_2 = 10^{-7}$, using the numerical fit for $m(r)$ given by Equation (64), with initial conditions $x(-5) = 0$, $y(-5) = -0.5$, $z(-5) = 0.5000134$ and $w(-5) = 0.05$. The behavior is compatible with the current cosmic observations on the evolution of density parameters. The obtained current densities are $\Omega_m(0) \simeq 0.3$, $\Omega_{DE}(0) \simeq 0.7$ and $\Omega_r(0) \simeq 10^{-4}$.

Numerical calculations show that as in the case of the (r, m)-plane in Figure 1, the evolution of the densities does not substantially change if we choose $\lambda_2 < 10^{-7}$ (including $\lambda_2 \sim 10^{-127}$ obtained after inflationary restrictions). This indicates that cosmological constraints on λ_2 are not as stringent as local gravity constraints. In Figure 3 we show the behavior of the effective and geometrical dark energy equations of state for this numerical sample.

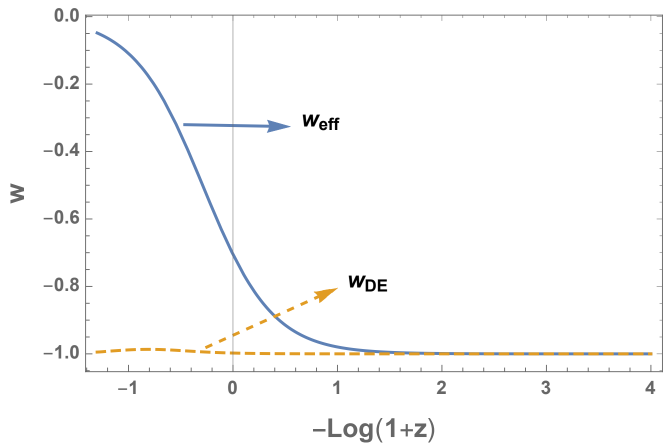

Figure 3. The effective equation of state w_{eff} and the equation of state associated with the geometric dark energy w_{DE} for the cosmological evolution of the density parameters described in Figure 2. The initial conditions lead to a scenario very close to the ΛCDM.

Please note that these numerical results are consistent with those obtained in [59], showing that the R^2 corrections in the matter era are negligible. The R^2 term is also consistent with local gravity tests according to the above numerical values of m. It is worth noting that if we continue lowering the values of η, the model becomes practically undistinguishable from ΛCDM, but the local gravity constraints become more relaxed in the sense that the scale μ does not have to be so small compared to H_0. Thus, we find the following behavior

$$\begin{aligned}
&(\eta = 10^{-8},\ p = 10^{8},\ \mu = 10^{-5}H_0) \quad \Rightarrow m = 5\times 10^{-25}\\
&(\eta = 10^{-10},\ p = 10^{10},\ \mu = 10^{-4}H_0) \quad \Rightarrow m = 5\times 10^{-25}\\
&(\eta = 10^{-10},\ p = 10^{10},\ \mu = 10^{-5}H_0) \quad \Rightarrow m = 5\times 10^{-27}\\
&(\eta = 10^{-12},\ p = 10^{12},\ \mu = 10^{-3}H_0) \quad \Rightarrow m = 5\times 10^{-25}\\
&(\eta = 10^{-12},\ p = 10^{12},\ \mu = 10^{-4}H_0) \quad \Rightarrow m = 5\times 10^{-27}
\end{aligned} \tag{65}$$

In this case, the local restrictions on m can be obtained for $\lambda_2 \lesssim 10^{-45}$.

Model 2.

A viable model with characteristics similar to those of the model (31) has the following form

$$f(R) = R - \left(2\lambda_1\mu^2 - \frac{\lambda_2}{\mu^2}R^2\right)e^{-\left(\frac{\mu^2}{R}\right)^{\eta}} \tag{66}$$

where as in the case of the model (31), $\lambda_1,\ \lambda_2 > 0$ and $0 < \mu \leq 1$. This model satisfies the limits

$$\lim_{R\to\infty} f(R) = R - 2\lambda_1\mu^2, \quad \lim_{R\to 0} f(R) = 0. \tag{67}$$

showing closeness to ΛCDM model with the cosmological constant vanishing in the flat spacetime. Let us first look at the model's ability to produce inflation. To this end we consider the model

$$f_1(R) = R + \frac{\lambda_2}{\mu^2}e^{-\left(\frac{\mu^2}{R}\right)^{\eta}}R^2 \tag{68}$$

where the second term in (66) was neglected. The corresponding scalar field in the Einstein frame has the form

$$\phi = \sqrt{\frac{3}{2}}\ln\left[1 + e^{-\left(\frac{\mu^2}{R}\right)^{\eta}}\lambda\left(\frac{\mu^2}{R}\right)\left(2+\eta\left(\frac{\mu^2}{R}\right)^{\eta}\right)\right]. \tag{69}$$

The scalar potential in the Einstein frame for $f(R)$ models

$$V(R(\phi)) = \frac{M_p^2}{2}\frac{Rf_1(R)_{,R} - f_1(R)}{(f_{1,R})^2}, \tag{70}$$

gives for the model (68)

$$V = \frac{\mu^2 M_p^2}{2}\frac{\lambda_2\left(\frac{R}{\mu^2}\right)^2\left[1+\eta\left(\frac{\mu^2}{R}\right)^{\eta}\right]e^{\left(\frac{\mu^2}{R}\right)^{\eta}}}{2\left[\lambda_2\left(\frac{R}{\mu^2}\right)\left(2+\eta\left(\frac{\mu^2}{R}\right)^{\eta}\right)+e^{\left(\frac{\mu^2}{R}\right)^{\eta}}\right]^2} \tag{71}$$

Using parametric method, in Figure 4 we show the shape of the potential, which maintains similarity with the Starobinsky potential and is appropriate for slow-roll inflation. The slow-roll parameters defined for the potential

$$\epsilon_v = \frac{M_p^2}{2}\left(\frac{V_{,\phi}}{V}\right)^2 \quad \textit{and} \quad \eta_v = M_p^2\frac{V_{,\phi\phi}}{V}, \tag{72}$$

take the following form using the variable $y = R/\mu^2$

$$\epsilon_v = \frac{\left(e^{1/y^\eta} - \eta\lambda_2 y^{1-\eta}\right)}{3\lambda_2^2 y^2 \left(1+\eta y^{-\eta}\right)^2}, \tag{73}$$

$$\eta_v = \frac{2e^{2/y^\eta} - 2\lambda_2 y e^{1/y^\eta}\left(4+2\eta y^{-\eta}\left(7-3\eta(1-y^{-\eta})\right)\right) + 2\eta^2\lambda_2^2 y^{2-\eta}\left(2+(2-\eta)y^{-\eta}+\eta y^{-2\eta}\right)}{3\lambda_2^2 y^2\left(1+\eta y^{-\eta}\right)\left(2+\eta y^{-\eta}\left(3-\eta(1-y^{-\eta})\right)\right)}. \tag{74}$$

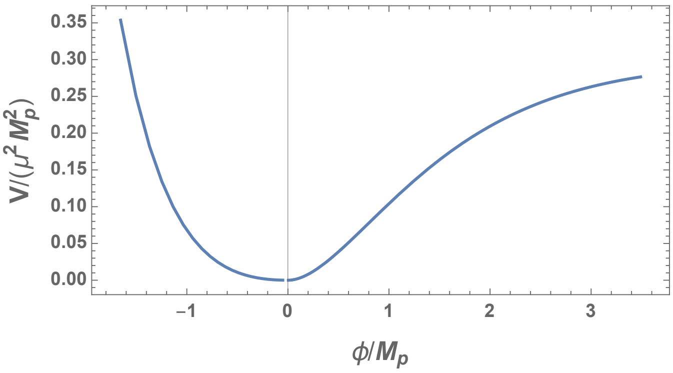

Figure 4. The scalar field potential in the Einstein frame for the model (68) for $\eta = 0.03$, $\lambda_2 = 1$. It can be observed that the potential has the appropriate behavior to develop slow-roll inflation.

These parameters are evaluated at the horizon crossing where the curvatures takes the value R_i, i.e., $y = y_i$. The inflaton value at the end of inflation is found from the condition $\epsilon_v(y_e) \simeq 1$, which leads to the approximate equation for y_e

$$1 - \eta\lambda y^{1-\eta} \simeq \sqrt{3}\lambda y\left(1+\eta y^{-\eta}\right) \tag{75}$$

where we neglected the exponential for $y >> 1$. Additionally if we consider $\eta << 1$, then $y^{1-\eta} \sim y$ and we ca appreciate the magnitude of the curvature at the end of inflation from

$$y_e \sim \frac{1}{\eta + \sqrt{3}(1+\eta)}\frac{1}{\lambda_2} \sim \frac{1}{\sqrt{3}\lambda_2}. \tag{76}$$

In the slow-roll approximation the duration of inflation is measured by the e-folding number N

$$N \simeq \frac{1}{M_p^2}\int_{\phi_e}^{\phi_i}\frac{V}{V_{,\phi}}d\phi = \frac{3}{2}\lambda_2^2\int_{y_e}^{y_i}\frac{y\left(1+\eta y^{-\eta}\right)\left(2+\eta y^{-\eta}\left(3-\eta(1-y^{-\eta})\right)\right)}{\left(1-\eta\lambda_2 y^{1-\eta}\right)\left(1+\lambda_2 y\left(2+\eta y^{-\eta}\right)\right)}dy, \tag{77}$$

where y_i is the curvature at the horizon crossing. Numerical integration gives y_i for a given number of e-foldings before the end of inflation, sufficient to prove the viability of the model to predict the values of inflationary observables. The spectral index of scalar perturbations and the tensor-to-scalar ratio are among the most important observables and for the potential driven inflation are given in therms of the slow-roll parameters by

$$n_s = 1 - 6\epsilon_v + 2\eta_v, \quad and \quad r = 16\epsilon_0. \tag{78}$$

To evaluate n_s and r we will consider the case with numerical parameters that were used to obtain the evolution of density parameters in Figure 2 ($\eta = 0.01$) (dotted line in Figure 1) and that satisfy local gravity constraints ($\mu = 10^{-8}H_0$) and $\lambda_2 = 10^{-127}$ from (53). We can use these results from the model (31) because the intermediate matter era and the late time behavior is the same for both models, including the local gravity restrictions. After numerical calculations, taking $y_e = 6.06 \times 10^{126}$

(suggested by (76)) and $N \approx 55$ we find that $y_i \approx 3.87 \times 10^{128}$ which gives, after replacing in (73) and (74),

$$n_s \approx 0.963 \quad and \quad r \approx 0.0038, \tag{79}$$

which are in good agreement with the current Planck observations. From (69) we find $\phi_e \approx 0.93 M_p$ and $\phi_i \approx 5.28 M_p$. The corresponding Hubble parameter during inflation is $H_i \approx 5.7 \times 10^{13}$ $Gev \sim 2.3 \times 10^{-5} M_p$. Then the model is capable of describing inflation, matter era and late time accelerated expansion.

To analyze the stability conditions we first define the constant λ_1 in such a way that the de Sitter solution at $r = -2$ is reached at $R = R_1$. The r and m parameters take the form

$$r = -\frac{y^{1+\eta} e^{1/y^\eta} - 2\eta\lambda_1 + \lambda_2 y^2 \left(\eta + 2y^\eta\right)}{y^{1+\eta} e^{1/y^\eta} - 2\lambda_1 y^\eta + \lambda_2 y^{2+\eta}} \tag{80}$$

$$m = \frac{2\eta\lambda_1 \left((1+\eta)y^\eta - \eta\right) + \lambda_2 \left(2y^{2\eta+2} + 3\eta y^{\eta+2} + \eta^2 y^2 \left(1 - y^\eta\right)\right)}{y^\eta \left(\lambda_2 y^2 \left(2y^\eta + \eta\right) + y^{\eta+1} e^{1/y^\eta} - 2\eta\lambda_1\right)} \tag{81}$$

where $y = R/\mu^2$. The equation $r = -2$ at $R = R_1$ ($y = y_1$) gives

$$\lambda_1 = \frac{y_1^{\eta+1} e^{1/y_1^\eta} - \eta\lambda_2 y_1^2}{4y_1^\eta - 2\eta}, \tag{82}$$

which lead to $\lambda_1 > 0$ for

$$y_1^\eta > \frac{\eta}{2}, \quad and \quad \lambda_2 < \frac{1}{\eta} y_1^{\eta-1} e^{1/y_1^\eta}. \tag{83}$$

Replacing λ_1 in m (81), the stability condition for de Sitter point, $0 < m(r = -2) \leq 1$ leads to the inequality

$$0 < \frac{\eta e^{1/y_1^\eta} \left((1+\eta)y_1^\eta - \eta\right) + 2\lambda_2 y_1 \left(2y_1^{2\eta} + \eta(2-\eta)y_1^\eta - \eta^2\right)}{2y_1^\eta \left(e^{1/y_1^\eta} \left(y_1^\eta - \eta\right) + 2\lambda_2 y_1^{1+\eta}\right)} \leq 1. \tag{84}$$

To facilitate the numerical analysis, in what follows we will set $y_1 = 1$, equivalent to $R_1 = \mu^2$. Setting $y_1 = 1$ in (84) we find

$$0 < \frac{e\eta + 4\lambda_2 \left(1 + \eta - \eta^2\right)}{2e(1-\eta) + 4\lambda_2} \leq 1 \quad \Rightarrow \quad 0 < \eta \leq \frac{3e + 4\lambda_2}{8\lambda_2} - \frac{1}{8\lambda_2}\sqrt{9e^2 - 8e\lambda_2 + 16\lambda_2^2} \tag{85}$$

which given the fact that $0 < \eta \leq 1$, is satisfied by any $\lambda_2 > 0$. The first derivative of $f(R)$, after replacing λ_1 and setting $y_1 = 1$ becomes

$$f_{,R} = e^{-1/y^\eta} \left[e^{1/y^\eta} + \lambda_2 y \left(\frac{\eta}{y^\eta} + 2\right) + \frac{\eta^2\lambda_2}{(2-\eta)y^\eta} - \frac{e\eta}{(2-\eta)y^\eta}\right] \tag{86}$$

Since all the terms, except the last one, are positive then to satisfy the condition $f_{,R} > 0$ it is enough that it is fulfilled

$$e^{1/y^\eta} - \frac{e\eta}{(2-\eta)y^\eta} > 0 \tag{87}$$

Since $e^{1/y^\eta} > 1$, and $y > 1$ then the sufficient condition to satisfy $f_{,R} > 0$ is

$$\eta < \frac{2}{1+e}. \tag{88}$$

Repeating the same procedure with $f_{,RR}$ we find

$$f_{,RR} = \frac{1}{\mu^2} e^{-\frac{1}{y^\eta}} \left[\lambda_2 \left(\eta^2 \frac{1}{y^{2\eta}} + \eta(3-\eta) \frac{1}{y^\eta} + 2 \right) + \frac{\eta(e - \eta\lambda_2)}{2-\eta} \left(1 + \eta - \eta \frac{1}{y^\eta} \right) \frac{1}{y^{2+\eta}} \right] \tag{89}$$

which automatically satisfies $f_{,RR} > 0$ since $0 < \eta \leq 1$, $y > 1$ and, according to (83), $\lambda_2 < e/\eta$. Then the model (66) satisfies all conditions of stability and cosmological viability.

Concerning the local gravity restrictions, for the solar system the model gives the same values for m shown in (63) and (65). Likewise the density parameters and the equation of state, present the same behavior as shown in Figures 2 and 3. As is the case for most of the realistic models, the stringent local gravity constraints forces the models (31) and (66) to be practically indistinguishable form ΛCDM. The possibility remains that further analysis of matter perturbations allows finding a departure from ΛCDM.

The exponential term in the models (31) and (66) is useful to avoid some type of singularities. Excluding the last term in (31) and (66) we can see that $f(R) \to R - 2\mu^2\Lambda$ as $R \to \infty$, $f_{,R}(R \to \infty)$ tends to 1 and $f_{,RR}, f_{,RRR}, ... \to 0$ at $R \to \infty$. Then the r.h.s. of Equation (4), excluding the matter density, for the models (31) and (66), which gives the corresponding ρ_{eff}, tends to a constant value on singular solutions with $R \to \infty$, avoiding in this way the appearance of type I and type III future singularities [37]. From Figures 1 and 2 it is clear also that the inflationary term in the models (31) and (66) does not have any influence on the stability of matter era.

4. Discussion

Two models of modified gravity that are able to explain early time inflation and late time accelerated expansion were studied. The models include an exponential function of de form $e^{-(\mu^2/R)^\eta}$ and the R^2 term. The factor $e^{-(\mu^2/R)^\eta}$, which is present in both models, leads to the limit $f(R) \to 0$ at $R \to 0$ implying the disappearance of the cosmological constant. i.e., the models contain the flat space-time solution. The stability, cosmological viability and local gravity restrictions were studied. The dynamical system was solved under appropriate initial conditions, and the cosmological evolution for the density parameters corresponding to radiation, matter and (geometrical) dark energy was obtained, which is closely adjusted to current observations. Consequently, the equation of state evolves according to observations with w_{eff} showing the transition to the accelerated phase at the currently observed $z_t \sim 0.5$, and $w_{DE} \simeq -1$.

The local gravity constraints, as expected, impose very stringent conditions for m to achieve values of the order $m \lesssim 10^{-24}$, which demand very small values for the scale μ ($\mu \sim 10^{-8} H_0$), although this scale may increase as we take smaller values of η. However, at the same time, making η smaller brings the model closer to ΛCDM, making it practically indistinguishable from it. In any case the general result is that the stronger the local gravity restrictions are, the further in the future the final de Sitter attractor of the system is. It is also interesting to note that the numerical results for local restrictions on m can be obtained for $\lambda_2 \lesssim 10^{-55}$, even though λ_2 is subject to the restriction (53) which results in much smaller values than this limit. On the other hand, the cosmological constraints, which do not depend on the scale μ, impose softer conditions on λ_2, being sufficient to consider $\lambda_2 \lesssim 10^{-7}$.

The expressions for m given by (51) for the model (31) and by (81) for the model (66) suggest a correlation between the curvature dependent parameter m and λ_2, which could be useful to fix λ_2 by local gravity constraints on m. This is an interesting alternative mechanism to fix λ_2, other than the condition (53) where the mass M^2 is determined from the amplitude of the scalar power spectrum. On the other hand, at high curvature typical of inflation, the model (31) leads to the Starobinsky inflation while the model (66) gives a new potential with the appropriate behavior to develop successful slow-roll inflation. A peculiarity of this potential is its dependence on η and λ_2 that is transferred to the slow-roll parameters, allowing exploring a wider region of possibilities for the inflationary observables, compared to the Starobinsky potential.

A more detailed analysis of local gravity restrictions is necessary, particularly to test whether local gravity constraints can independently and uniquely determine a value of λ_2 that is consistent with inflation. Further study of cosmological effects that distinguish the models form ΛCDM is needed, for instance, the evolution of the background and matter density perturbations which could give patterns in the growth of structures that mark the difference with ΛCDM.

Funding: This research received no external funding.

Acknowledgments: This work was supported by Universidad del Valle under project CI 71195.

Conflicts of Interest: The author declare no conflict of interest.

References

1. Copeland, E.J.; Sami, M.; Tsujikawa, S. Dynamics of dark energy. *Int. J. Mod. Phys. D* **2006**, *15*, 753–1936. [CrossRef]
2. Sahni, V. Dark Matter and Dark Energy. *Lect. Notes Phys.* **2004**, *653*, 141–180.
3. Padmanabhan, T. Cosmological Constant-the Weight of the Vacuum. *Phys. Rep.* **2003**, *380*, 235–320. [CrossRef]
4. Bamba, K.; Capozziello, S.; Nojiri, S.; Odintsov, S.D. Dark energy cosmology: The equivalent description via different theoretical models and cosmography tests. *Astrophys. Space Sci.* **2012**, *342*, 155–228. [CrossRef]
5. Dolgov, A.D.; Kawasaki, M. Can modified gravity explain accelerated cosmic expansion? *Phys. Lett. B* **2003**, *573*, 1–4. [CrossRef]
6. Nojiri, S.; Odintsov, S.D. Introduction to Modified Gravity and Gravitational Alternative for Dark Energy. *Int. J. Geom. Meth. Mod. Phys.* **2007**, *4*, 115–146. [CrossRef]
7. Amendola, L.; Polarski, D.; Tsujikawa, S. Are f(R) dark energy models cosmologically viable? *Phys. Rev. Lett.* **2007**, *98*, 131302. [CrossRef]
8. Capozziello, S.; Tsujikawa, S. Solar system and equivalence principle constraints on f(R) gravity by chameleon approach. *Phys. Rev. D* **2008**, *77*, 107501. [CrossRef]
9. Sotiriou, T.P.; Faraoni, V. f(R) Theories Of Gravity. *Rev. Mod. Phys.* **2010**, *82*, 451–497. [CrossRef]
10. Tsujikawa, S. Modified gravity models of dark energy. *Lect. Notes Phys.* **2010**, *800*, 99–145.
11. Nojiri, S.; Odintsov, S.D. Accelerating cosmology in modified gravity: From convenient F(R) or string-inspired theory to bimetric F(R) gravity. *Int. J. Geom. Meth. Mod. Phys.* **2014**, *11*, 1460006. [CrossRef]
12. Capozziello, S. Curvature Quintessence. *Int. J. Mod. Phys. D* **2002**, *11*, 483–492. [CrossRef]
13. Capozziello, S.; Carloni, S.; Troisi, A. Quintessence without scalar fields. *Recent Res. Dev. Astron. Astrophys.* **2003**, *1*, 625.
14. Nojiri, S.; Odintsov, S.D. Where new gravitational physics comes from: M-theory? *Phys. Lett. B* **2003**, *576*, 5–11. [CrossRef]
15. Nojiri, S.; Odintsov, S.D. Modified gravity with negative and positive powers of the curvature: Unification of the inflation and of the cosmic acceleration. *Phys. Rev. D* **2003**, *68*, 123512. [CrossRef]
16. Carroll, S.M.; Duvvuri, V.; Trodden, M.; Turner, M.S. Is Cosmic Speed-Up Due to New Gravitational Physics? *Phys. Rev. D* **2004**, *70*, 043528. [CrossRef]
17. Faraoni, V. The stability of modified gravity models. *Phys. Rev. D* **2005**, *72*, 124005. [CrossRef]
18. De la Cruz-Dombriz, A.; Dobado, A. A f(R) gravity without cosmological constant. *Phys. Rev. D* **2006**, *74*, 087501. [CrossRef]
19. Brookfield, A.W.; van de Bruck, C.; Hall, L.M.H. Viability of f (R) Theories with Additional Powers of Curvature. *Phys. Rev. D* **2006**, *74*, 064028. [CrossRef]
20. Li, B.; Barrow, J.D. The Cosmology of f(R) Gravity in the Metric Variational Approach. *Phys. Rev. D* **2007**, *75*, 084010. [CrossRef]
21. Abdalla, M.C.B.; Nojiri, S.; Odintsov, S.D. Consistent modified gravity: Dark energy, acceleration and the absence of cosmic doomsday. *Class. Quant. Grav.* **2005**, *22*, L35. [CrossRef]
22. Cognola, G.; Elizalde, E.; Nojiri, S.; Odintsov, S.D.; Zerbini, S. One-loop f(R) gravity in de Sitter universe. *JCAP* **2005**, *502*, 010. [CrossRef]
23. Capozziello, S.; Cardone, V.F.; Troisi, A. Reconciling dark energy models with f(R) theories. *Phys. Rev. D* **2005**, *71*, 043503. [CrossRef]

24. Allemandi, G.; Borowiec, A.; Francaviglia, M.; Odintsov, S.D. Dark Energy Dominance and Cosmic Acceleration in First Order Formalism. *Phys. Rev. D* **2005**, *72*, 063505. [CrossRef]
25. Koivisto, T.; Kurki-Suonio, H. Cosmological perturbations in the Palatini formulation of modified gravity. *Class. Quant. Grav.* **2006**, *23*, 2355–2369. [CrossRef]
26. Brevik, I. Crossing of the $w = -1$ barrier in viscous modified gravity. *Int. J. Mod. Phys. D* **2006**, *15*, 767–776. [CrossRef]
27. Nojiri, S.; Odintsov, S.D. Modified f(R) gravity consistent with realistic cosmology: From matter dominated epoch to dark energy universe. *Phys. Rev. D* **2006**, *74*, 086005. [CrossRef]
28. Capozziello, S.; Nojiri, S.; Odintsov, S.D.; Troisi, A. Cosmological viability of f(R)-gravity as an ideal fluid and its compatibility with a matter dominated phase. *Phys. Lett. B* **2006**, *639*, 135–143. [CrossRef]
29. Nojiri, S.; Odintsov, S.D. Modified gravity as an alternative for Lambda-CDM cosmology. *J. Phys. A* **2007**, *40*, 6725-6732. [CrossRef]
30. Olmo, G.J. Limit to General Relativity in f(R) theories of gravity. *Phys. Rev. D* **2007**, *75*, 023511. [CrossRef]
31. Hu, W.; Sawicki, I. Models of f(R) Cosmic Acceleration that Evade Solar-System Tests. *Phys. Rev. D* **2007**, *76*, 064004. [CrossRef]
32. Starobinsky, A.A. A new type of isotropic cosmological models without singularity. *Phys. Lett. B* **1980**, *91*, 99–102. [CrossRef]
33. Starobinsky, A.A. Disappearing cosmological constant in f(R) gravity. *JETP Lett.* **2007**, *86*, 157–163. [CrossRef]
34. Appleby, S.A.; Battye, R.A. Do consistent F(R) models mimic General Relativity plus Λ? *Phys. Lett. B* **2007**, *654*, 7–12. [CrossRef]
35. Nojiri, S.; Odintsov, S.D. Newton law corrections and instabilities in f(R) gravity with the effective cosmological constant epoch. *Phys. Lett. B* **2007**, *652*, 343–348. [CrossRef]
36. Cognola, G.; Elizalde, E.; Nojiri, S.; Odintsov, S.D.; Sebastiani, L.; Zerbini, S. Class of viable modified f(R) gravities describing inflation and the onset of accelerated expansion. *Phys. Rev. D* **2008**, *77*, 046009. [CrossRef]
37. Elizalde, E.; Nojiri, S.; Odintsov, S.D.; Sebastiani, L.; Zerbini, S. Non-singular exponential gravity: A simple theory for early- and late-time accelerated expansion. *Phys. Rev. D* **2011**, *83*, 086006. [CrossRef]
38. Bamba, K.; Nojiri, S.; Odintsov, S.D. Future of the universe in modified gravitational theories: Approaching to the finite-time future singularity. *J. Cosmol. Astropart. Phys.* **2008**, *810*, 045. [CrossRef]
39. Barrow, J.D.; Clifton, T. Exact cosmological solutions of scale-invariant gravity theories. *Class. Quant. Grav.* **2005**, *23*, L1. [CrossRef]
40. Clifton, T.; Barrow, J.D. Further Exact Cosmological Solutions to Higher-Order Gravity Theories. *Class. Quant. Grav.* **2006**, *23*, 2951. [CrossRef]
41. Capozziello, S.; de Felice, A. f(R) cosmology by Noether's symmetry. *J. Cosmol. Astropart. Phys.* **2008**, *808*, 016. [CrossRef]
42. Capozziello, S.; Stabile, A.; Troisi, A. Spherically symmetric solutions in f(R)-gravity via Noether Symmetry Approach. *Class. Quant. Grav.* **2007**, *24*, 2153–2166. [CrossRef]
43. Capozziello, S.; Stabile, A.; Troisi, A. Spherical symmetry in f(R)-gravity. *Class. Quant. Grav.* **2008**, *25*, 085004. [CrossRef]
44. Barrow, J.D.; Cotsakis, S. Inflation and the conformal structure of higher-order gravity theories. *Phys. Lett. B* **1988**, *214*, 515–518. [CrossRef]
45. Nojiri, S.; Odintsov, S.D. Modified Gauss-Bonnet theory as gravitational alternative for dark energy. *Phys. Lett. B* **2005**, *631*, 1–6. [CrossRef]
46. Nojiri, S.; Odintsov, S.D.; Gorbunova, O.G. Dark energy problem: From phantom theory to modified Gauss-Bonnet gravity. *J. Phys. A* **2006**, *39*, 6627–6634. [CrossRef]
47. Cognola, G.; Elizalde, E.; Nojiri, S.; Odintsov, S.D.; Zerbini, S. Dark energy in modified Gauss-Bonnet gravity: Late-time acceleration and the hierarchy problem. *Phys. Rev. D* **2006**, *73*, 084007. [CrossRef]
48. Nojiri, S.; Odintsov, S.D. Unifying inflation with LambdaCDM epoch in modified f(R) gravity consistent with Solar System tests. *Phys. Lett. B* **2007**, *657*, 238. [CrossRef]
49. Nojiri, S.; Odintsov, S.D. Modified f(R) gravity unifying R^m inflation with ΛCDM epoch. *Phys. Rev. D* **2008**, *77*, 026007. [CrossRef]
50. Odintsov, S.D.; Saez-Chillon, D.; Sharov, G.S. Is exponential gravity a viable description for the whole cosmological history? *Eur. Phys. J. C* **2017**, *77*, 862. [CrossRef]

51. Odintsov, S.D.; Saez-Chillon, D.; Sharov, G.S. Testing logarithmic corrections on R^2-exponential gravity by observational data. *Phys. Rev. D* **2019**, *99*, 024003. [CrossRef]
52. Odintsov, S.D.; Oikonomou, V.K. Unification of Constant-roll Inflation and Dark Energy with Logarithmic R^2-corrected and Exponential F(R) Gravity. *Nucl. Phys. B* **2017**, *923*, 608–632. [CrossRef]
53. Li, B.; Barrow, J.D.; Mota, D.F. The Cosmology of Modified Gauss-Bonnet Gravity. *Phys. Rev. D* **2007**, *76*, 044027. [CrossRef]
54. Oikonomou, V.K. Singular Bouncing Cosmology from Gauss-Bonnet Modified Gravity. *Phys. Rev. D* **2015**, *92*, 124027. [CrossRef]
55. Amendola, L.; Gannouji, R.; Polarski, D.; Tsujikawa, S. Conditions for the cosmological viability of f(R) dark energy models. *Phys. Rev. D* **2007**, *75*, 083504. [CrossRef]
56. Tsujikawa, S. Observational signatures of f(R) dark energy models that satisfy cosmological and local gravity constraints. *Phys. Rev. D* **2008**, *77*, 023507. [CrossRef]
57. Rausan, R.; Chaubey, R. Finsler-Randers cosmology in the framework of a particle creation mechanism: A dynamical systems perspective. *Eur. Phys. J. Plus* **2020**, *135*, 228. [CrossRef]
58. Papagiannopoulos, G.; Basilakos, S.; Paliathanasis, A.; Savvidou, S.; Stavrinos, P.C. Finsler-Randers cosmology: Dynamical analysis and growth of matter perturbations. *Class. Quantum Gravity* **2017**, *34*, 22. [CrossRef]
59. Granda, L.N. Modified gravity with an exponential function of curvature. *arXiv* **2020**, arXiv:2003.09006.